XX. NEUROLOGY*

L. Stark
J. F. Dickson III
G. Cook
D. Martin
G. A. Masek
J. A. Michael
H. Miyahara
A. Natapoff
J. Negrete
O. Sanchez-Felipe
A. A. Sandberg
S. F. Stanten
T. Webb
G. H. Whipple
G. N. Yankelevich
B. L. Zuber

A. MICROSACCADES AND THE VELOCITY-AMPLITUDE RELATIONSHIP FOR SACCADIC EYE MOVEMENTS

It has been known for some time that the velocity of a saccadic eye movement is dependent upon its amplitude.[1-3] This relationship is one of the nonlinearities encountered in a study of the versional eye movement system as a servomechanism.[4] Westheimer[1] has studied the relationship of maximum velocity to amplitude for voluntary saccades ranging from 2 to 30 degrees. His curve shows a curvilinear relationship over the entire range, with a tendency to saturation for larger amplitudes. Gurevich,[2] in studying average velocity, has found a similar relationship, although his velocities are much lower than Westheimer's, as would be expected. Gurevich also found that average velocity measurements for any given size movement were fairly constant under the following conditions: horizontal, diagonal or vertical movement; variation of starting position and direction of movement; in the presence of visible fixation points for the stimulus or in total darkness with conditioned eye movements. He also found that average velocities of secondary saccadic corrections fell on the same curve that he obtained for the types of movements described above. The range of amplitudes used in his study was from 1 to 35 degrees.

The data of Gurevich indicate that a single physiological system is responsible for a wide variety of saccadic eye movements. In an attempt to determine if microsaccades, the small (1 to 20 minutes of arc) involuntary saccades observed during fixation, are the output of this same system, we have made a study of the maximum velocity of such movements.

The apparatus for presenting a fixation point and calibration points at optical infinity, as well as the method of measuring these small eye movements, has been described[5] previously. The signal proportional to eye position was recorded on one channel of a recorder (Sanborn Model 320). This signal was also electronically differentiated and the derivative recorded on the other channel of the recorder. In an attempt to improve resolution, signals proportional to the pen positions on the eye position and velocity channels were recorded on a second recorder (Visicorder Model 1508). This provides a

*Major support for this research is provided by the U.S. Public Health Service (B-3055-4, B-3090-4, MH-06175-02), the U.S. Navy (Office of Naval Research (Nonr-1841 (70)), the U.S. Air Force (AF49(638)-1313), administered by the Electronic Systems Laboratory, M.I.T.

further amplification factor of approximately five. Thus two recorders were used, the Sanborn being primarily used to keep both signals on scale and to provide an immediate check on the linearity of calibrations. Visicorder records were used in all analyses.

Calibration of the velocity channel was accomplished by recording a triangular wave on the eye-position channel and its derivative on the velocity channel. All gains and calibrations were unchanged for this procedure. Thus, given the amplitude of the triangular wave on the eye-position channel and the frequency of the waveform, a velocity in degrees per second could be related to a given deflection on the velocity channel. Such

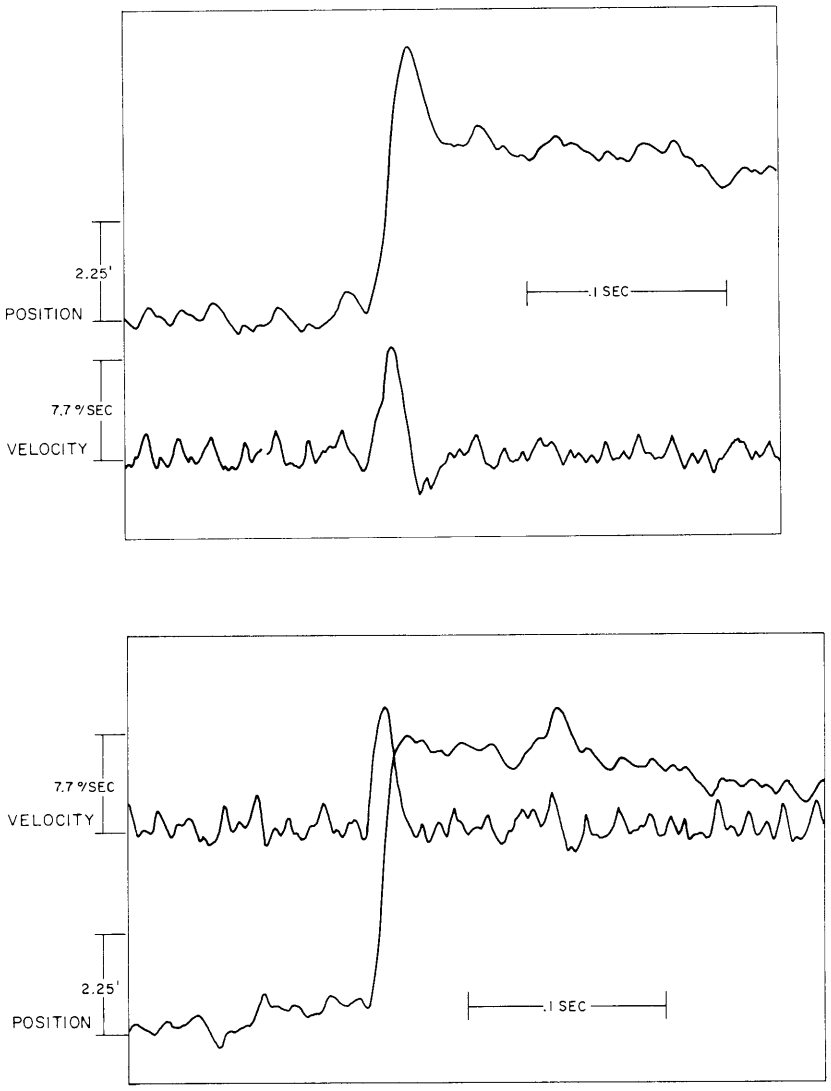

Fig. XX-1. Two typical microsaccades and their velocity traces. Note that although the two movements are approximately the same size, only one has overshoot.

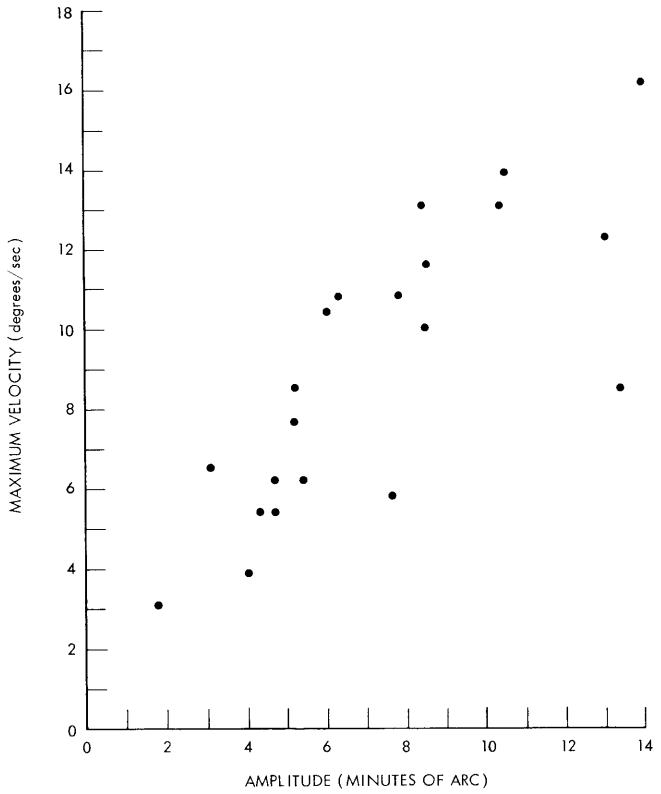

Fig. XX-2. Maximum velocity (degrees/second) vs amplitude (minutes of arc) for microsaccades.

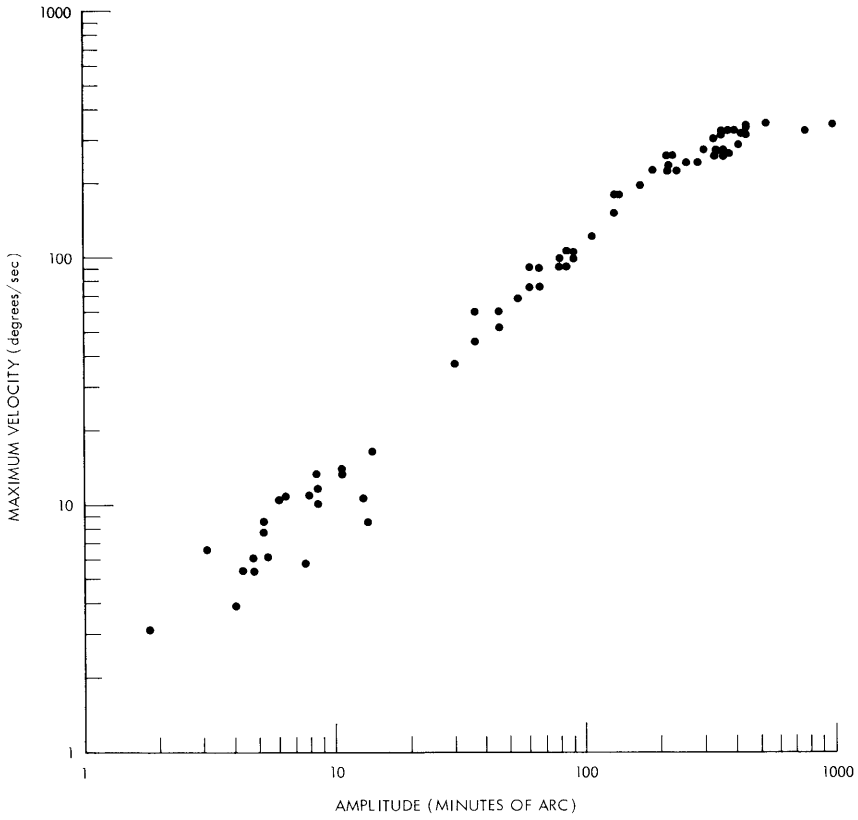

Fig. XX-3. Maximum velocity (degrees/second) vs amplitude (minutes of arc) for microsaccades, involuntary corrective saccades, and voluntary saccades.

calibrations were made for at least three frequencies within the range of velocities observed in the experiment.

Figure XX-1 shows some typical microsaccades and their velocity traces. Here we see two movements of roughly the same size, one with a great deal more overshoot than the other. Note that the overshoot is proportionately much greater than that normally seen with larger saccades. Figure XX-2 is a plot of maximum velocity in degrees per second (ordinate) as a function of amplitude in minutes of arc (abscissa). It is clear that velocity is an increasing function of amplitude for these movements.

In Fig. XX-3 we have replotted the data from Fig. XX-2 and added data points from larger voluntary saccades and secondary corrective saccades. The latter data were obtained in the same manner as those for the microsaccades, except, of course, that the stimulus conditions were different. The velocity data for the larger movements are very close to those of Westheimer.[1] The points are plotted on logarithmic scales because of the large ranges involved. A smooth continuous curve through all data points is clearly justified, and indicates, indeed, that microsaccades are produced by the same physiological system as voluntary saccades and involuntary corrective saccades.

It is interesting that so much overshoot is observed on microsaccades as compared with larger saccades. With further experiments designed to provide a dynamical model of this system, it is hoped that some explanation of this observation will be forthcoming.

We are indebted to Professor L. R. Young, of the Department of Aeronautics and Astronautics, M. I. T., who pointed out the need for velocity data on microsaccades.

B. L. Zuber, G. Cook, L. Stark

References

1. G. Westheimer, Mechanism of saccadic eye movements, A. M. A. Arch. Ophthalmol. 52, 710 (1954).

2. B. Kh. Gurevich, Universal characteristics of fixation eye jerks, Biofiz. 6, 377 (1961).

3. J. E. Hyde, Some characteristics of voluntary human ocular movements in the horizontal plane, Am. J. Ophthalmol. 48, 85 (1959).

4. L. R. Young and L. Stark, A discrete model for eye tracking movements, IEEE Trans. Vol. Mil-7, p. 113, 1963.

5. B. L. Zuber, A. Crider, and L. Stark, Saccadic suppression associated with microsaccades, Quarterly Progress Report No. 74, Research Laboratory of Electronics, M. I. T., July 15, 1964, p. 244.

B. HUMAN HORIZONTAL EYE-MOVEMENT MECHANISM

This report gives an account of a continuing investigation into the horizontal eye-movement mechanism, the first part of which was reported in Quarterly Progress

Report No. 76 (pages 343-352). Since the time of the first report, new evidence has brought about certain changes and additions in the model of the physical plant.

The updated model (Fig. XX-5) has been used with experimental data to determine the controller or driving-function behavior during saccadic movements. The minimum time behavior for the model has also been calculated and is compared with the actual behavior.

1. Physical Structure

a. Resting Length of Muscle

Robinson[1] describes measurements on the lateral rectus of a cat in which he finds the rest length to be approximately 25 mm. By extrapolation from a figure of Robinson,[2] one finds that the distance from the length of maximum tension to that of zero tension is approximately 12 mm. From Wilkie,[3] we find that this distance just described is Lo/2, where Lo is the length of the muscle for developing maximum tension. Therefore, $Lo/2 \approx 12$ mm, and Lo = 24 mm. So the rest length is approximately the same as Lo which means that if we look straight ahead, the operating point of the muscle is on the peak of the curve. See Fig. XX-4.

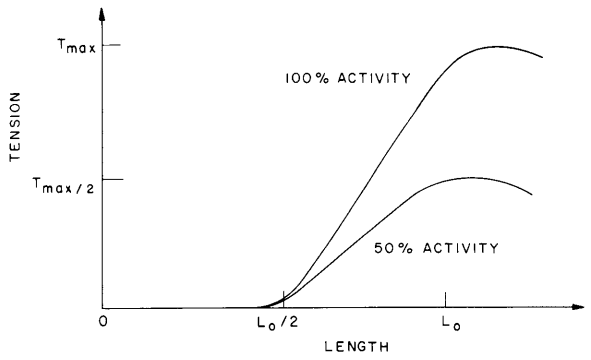

Fig. XX-4. Active muscle length-tension relationship.

This point brings up a question about stability, since the stretched muscle will now be operating with a negative spring coefficient. The shortened muscle, which is operating with a positive spring coefficient, is more highly activated and predominates, thereby ensuring stability at any resting position. As for the dynamic situation, during a movement toward center where the stretched muscle is more highly activated than the shortened one, incremental instability may exist. This means that for a given degree of activity the force pulling on the eye increases during the movement, although the eye is moving in the direction of the force. As the desired position is approached and the

activity of the stretched muscle falls off, the stable situation described above prevails.

A factor that lessens this temporary incremental stability is the flatness of the length-tension muscle characteristic in the neighborhood of the peak. Because the

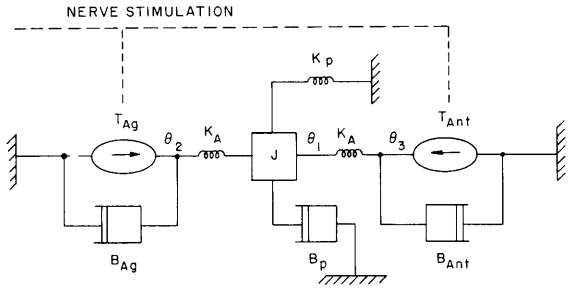

Fig. XX-5. Model of the physical system.

muscle does operate in this flat region, the contractile element is modeled as a tension source in parallel with nonlinear damping (Fig. XX-5).

b. Passive Tension

With the active muscles represented as tension sources with appropriate dynamics, the passive tension becomes important in bringing about an equilibrium of forces when the two muscles have different degrees of activity. From Ruch and Fulton,[4] we find the length tension slope of a relaxed muscle to be T_{max}/L_o. For the human, assuming $T_{max} \approx 500$ gm and $L_o \approx 4$ cm, we obtain $Kp \approx 125$ gm/cm; and since the radius of the eye is approximately 1 cm, $Kp \approx 2$ gm/degree.

c. Active Muscle Elasticity

Wilkie[3] states that at $T_o = T_{max}$, 3 per cent stretch occurs in the active muscle. For $T_{max} = 500$ grams, and a length of 4 cm, this yields a spring coefficient of

$$K_A = \frac{500 \text{ gram}}{0.03 \times 4 \text{ cm}},$$

or since 1 cm ≈ 1 rad, $K_A = 73$ grams/degree.

d. Active Damping

Hill,[5] who has spent many years studying muscle behavior, advanced the most accepted analytic description of a shortening active muscle behavior in the following equation:

$$v(T+a) = b(T_o - T),$$

where T is tension, v is velocity, T_o is static tension, and b is one-fourth the maximum shortening velocity of the muscle. This equation can be rearranged to yield

$$T = T_o - \left(\frac{T_o + a}{v + b}\right) v.$$

Now, $a \approx 0.25\, T_o$. Therefore

$$T = T_o - \left(\frac{1.25\, T_o}{v + b}\right) v,$$

and the active damping coefficient is

$$B_{Ag} = \frac{1.25\, T_o}{v + b}.$$

Here, T_o is the tension with zero velocity and with the muscle at length L_o. T_o increases with increased activity to a maximum value of T_{max}. We then see that the active damping coefficient of a shortening muscle is proportional to the degree of activity and is also a function of velocity.

It can be shown from the model, Fig. XX-5, that during an isometric contraction,

$$b = 0.25\, \frac{\dot{T}}{K_A}.$$

Now,

$$K_A = \frac{T_{max}}{0.3\, L},$$

where L is the rest length of the muscle. Therefore

$$b = 0.0075 \times \frac{\dot{T}}{T_{max}} \times L.$$

Assuming similar time behavior between cats and humans, we refer to Adler.[6] He shows an isometric contraction of a cat; $L \approx 2.5$ cm, $\dot{T}/T_{max} = 210$, and b = 3 rad/sec or 180°/sec. Recalling that 4b = maximum muscle velocity, we will take b = 250°/sec, since velocities as high as 800°/sec have been reported.

Katz[7] showed that the damping coefficient in an active muscle that is being lengthened is quite different from that in one that is shortening. It is still proportional to activity, but much larger than that for the shortening muscle and no longer a function of velocity.

From Katz[7] we find

$$B_{Ant} = \frac{12.5}{b}\, T_o.$$

Furthermore, Katz states that forces greater than 1.8 T_{max} in the lengthening muscle can damage the muscle. This factor will be an important consideration in calculating the minimum time behavior of the model.

e. Primary Position Tension

Breinin[8] shows a graph of integrated muscle potential vs eye position. Linearizing this curve, we obtain Fig. XX-6. For a 15° movement, the difference in tension

$$T_{Ag} - T_{Ant} = 15 \times Kp = 30 \text{ grams.}$$

In Fig. XX-6 this corresponds to 6.4-4.8, or 1.6 units on the ordinate. Inman et al.[9] found a linear relation between electric integral and tension with constant muscle length.

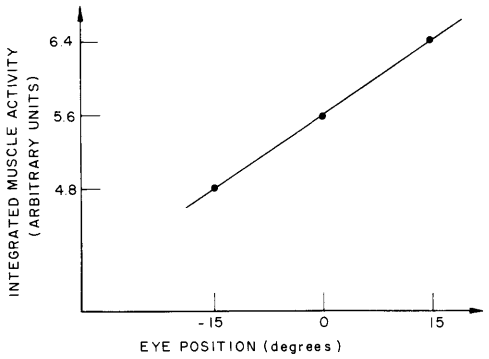

Fig. XX-6. Integrated muscle activity vs eye position.

We shall assume that the small length changes, 15°, do not invalidate this relation which we shall now utilize.

$$\frac{30 \text{ gm}}{1.6 \text{ units}} \times 5.6 \text{ units} = 105 \text{ grams.}$$

Thus, the tension in each muscle in the primary position, 0°, is approximately 100 grams.

f. Passive Damping

An experiment by Robinson[1] was used to determine the passive damping. The eye was activated for the zero-degree position, forced to the 4° position and released. Upon release, if we neglect inertia, it can be shown that $Bp\dot{\theta}(O) = Kp\theta(O)$.

With Kp = 2, $\theta(O) = 4$ and $\dot{\theta}(O) = 520°/\text{sec}$, we obtain Bp = 0.016 gram sec/degree.

For convenience, all the parameters of the system illustrated by Fig. XX-5 are tabulated:

$$B_{Ag} = T_{Ag}\left(\frac{1.25}{250 + \dot{\theta}_2}\right)\frac{\text{gram sec}}{\text{degree}}$$

$$B_{Ant} = T_{Ant}\,\frac{12.5}{250}\,\frac{\text{gram sec}}{\text{degree}}$$

$$K_A = 73 \text{ grams/degree}$$

$$Kp = 2 \text{ grams/degree}$$

$$Bp = 0.016 \text{ gram sec/degree}$$

$$J = 0.000047 \text{ gram sec}^2/\text{degree}.$$

2. Controller Behavior

The basic configuration is shown in Fig. XX-7. The target and output are known, and we would like to know the behavior of the control variable, U

$$W(U) = \theta_{out}$$

$$U = W^{-1}(\theta_{out}).$$

If W is known and if W^{-1} exists, then U can be found. Here, U is the nerve stimulation to the agonist and antagonist muscles.

This can be measured directly in the form of electromyograms. The accuracy and

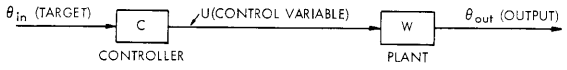

Fig. XX-7. System configuration.

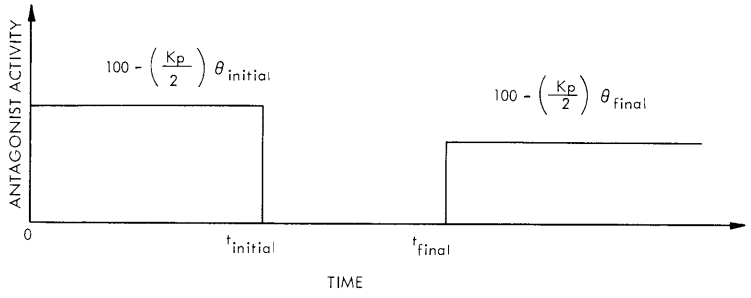

Fig. XX-8. Antagonist behavior during a saccadic movement.

readability of such measurements, however, leaves much to be desired, except in static situations.

Since W is known and W^{-1} exists, experimental output data can be used to calculate U. A problem does exist in that there are two unknowns, T_{Ag} and T_{Ant}. The electromyograms of the antagonist (see Davson[10]) are taken as the more readable of the two. On this basis, T_{Ant} is assumed to have the behavior shown in Fig. XX-8. This leaves T_{Ag} as the only unknown and it can be determined.

In the form assumed for T_{Ant}, we require that before the movement

$$T_{Ant} = 100 - \left(\frac{Kp}{2}\right)(\theta_{initial});$$

and after the movement,

$$T_{Ant} = 100 - \left(\frac{Kp}{2}\right)(\theta_{final}).$$

We also desire that during the movement, $T_{Ant} \approx 0$.

This was programmed on the computer first by generating a function g_1 such as that shown in Fig. XX-9 with the corners coming right after the start of the movement and right before the end of the movement. This function g_1 was then divided by $1 + K\dot{\theta}$ to yield g_2; that is, $g_2 = \frac{g_1}{1 + K\dot{\theta}}$. K was taken to be of such size as to cause g_2 to be very small throughout the movement.

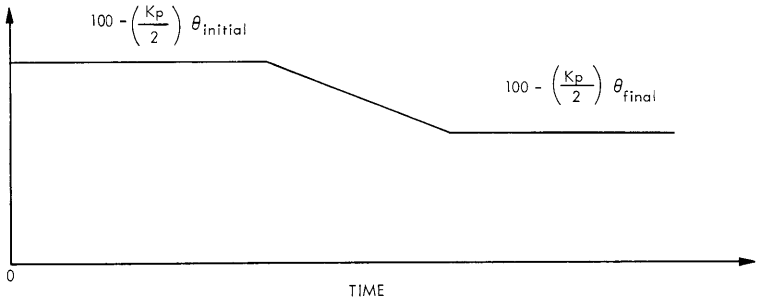

Fig. XX-9. g_1 artificial function used in generating T_{Ant}.

The behavior of T_{Ant} is shown in Fig. XX-10, together with the resulting behavior of T_{Ag}. It is seen that sometimes there is a burst of activity in T_{Ant} toward the end of the movement. This is caused by overshoot in the movement ($\dot{\theta}$ going negative) and

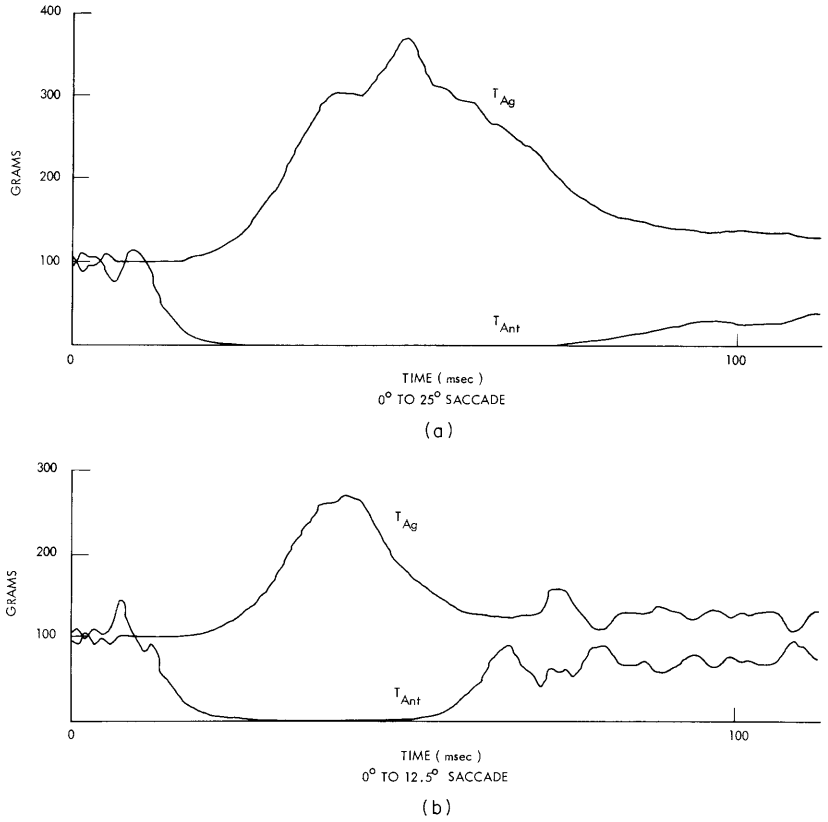

Fig. XX-10. Computed controller behavior during saccadic movements.

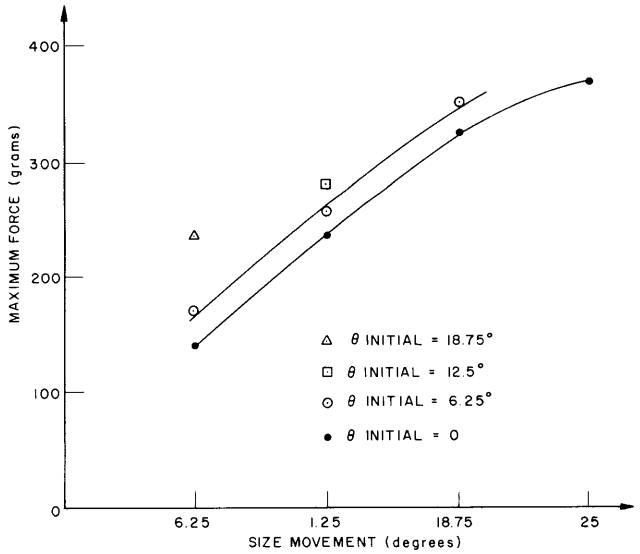

Fig. XX-11. Computed maximum force during saccadic movements.

by the way g_2 is generated, that is,

$$g_2 = \frac{g_1}{1 + K\theta}.$$

Davson[10] reports that such bursts have been observed in the antagonist, and, for this reason, no attempt was made to remove the peak.

The reciprocal innervation is well displayed here. The maximum force applied by the agonist for various movements is tabulated below and displayed in Fig. XX-11.

Movement (degrees)	Max T_{Ag} (grams)
0 to 6.25	143
0 to 12.5	240
0 to 18.75	323
0 to 25.0	369
6.25 to 12.5	172
6.25 to 18.75	254
6.25 to 25.0	337
12.5 to 25.0	283
18.75 to 25.0	243

3. Minimum Time Behavior

The control function that would be applied to the system to attain a given state in minimum time has been determined. Position and velocity plots, together with a phase trajectory for such a movement, are shown in Fig. XX-12. These data were obtained through computer simulation. The control behavior during these movements is as follows:

$$T_{Ag}[O, t_1) = 100 + \frac{Kp}{2}\,\theta_{initial}$$

$$T_{Ag}[t_1, t_s) = 500 \text{ grams } (T_{Ag}\,max)$$

$$T_{Ag}[t_s, t_2) = O$$

$$T_{Ag}[t_2, \infty) = 100 = \left(\frac{Kp}{2}\right)\theta_{final}$$

$$T_{Ant}[O, t_1) = 100 - \left(\frac{Kp}{2}\right)\theta_{initial}$$

$$T_{Ant}[t_1, t_s) = O$$

$$T_{Ant}[t_s, t_2) = 500 \text{ grams } (T_{Ant}\,max)$$

$$\text{if } \dot{\theta} \leq 16°/\text{sec}$$

$$T_{Ant}[t_s, t_2) = \frac{720}{1 + \frac{\dot{\theta}}{20}}$$

$$\text{if } \dot{\theta} > 16°/\text{sec}$$

(Recall $T_{Ant}\left(1 + \frac{\dot{\theta}}{20}\right) \leq 720$ to prevent muscle damage.)

$$T_{Ant}[t_2, \infty] = 100 - \left(\frac{Kp}{2}\right)\theta_{final}.$$

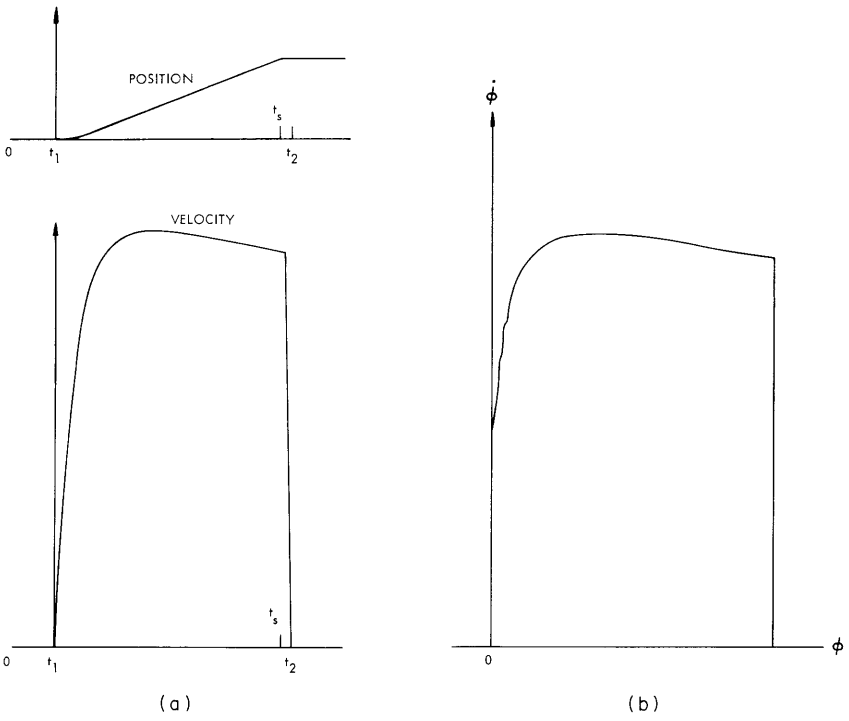

Fig. XX-12. (a) Minimum time plots. (b) Phase trajectory.

Tabulated below is a comparison of the actual eye movement behavior and the minimum time behavior.

Actual Behavior		Minimum Time Behavior	
Movement (degrees)	Time (msec)	Movement (degrees)	Time (msec)
0 to 6.25	35	0-6.6	9.4
0 to 12.5	52	0-13.6	18.8
0 to 18.75	65	0-21.8	32.6
0 to 25	94	0-28.2	43.8
6.25 to 12.5	35	6.3-12.2	9.4
6.25 to 18.75	56	6.3-18.6	18.8
6.25 to 25	73	6.3-26.1	32.6
		12.5-18	9.8
12.5 to 25	60	12.5-24	19.4
18.75 to 25	44	18.75-23.9	10.1

It is evident that the actual behavior of the system requires from 2 to 4 times as much time to execute a movement as would be the case if the system were minimizing time. It would be of interest to compare the actual system behavior with that which would result if other cost functions were minimized. Another consideration is that there may be transient processes between the nerve stimulation and the variables T_{Ag} and T_{Ant} of Fig. XX-5.

G. Cook, L. Stark

References

1. D. A. Robinson, The mechanics of human saccadic eye movement, J. Physiol. 174, 245-264 (1964).

2. Ibid., see Fig. 8, p. 254.

3. D. R. Wilkie, Facts and theories about muscle, Progress in Biophysics and Biophysical Chemistry, Vol. 4, pp. 294; 314, 1954.

4. Ruch and Fulton, Medical Physiology and Biophysics (W. B. Saunders Company, Philadelphia and London), p. 108.

5. A. V. Hill, J. Physiol. 93, 4 (1938).

6. F. H. Adler, Physiology of the Eye (The C. V. Mosby Company, St. Louis, 1959), p. 363.

7. B. Katz, The relation between force and speed in muscular contraction, J. Physiol. 96, 56 (1939).

8. G. M. Breinin, Analytic studies of the electromyogram of human extraocular muscle, Am. J. Ophthalmol. 46, Part II, 131 (September 1958).

9. Inman et al., Relation of human electromyogram to muscular tension, E. E. G. Clin. Neurophysiol. 4, 187-194 (1952).

10. H. Davson, The Eye, Vol. 3 (Academic Press, New York and London, 1962), p. 159.

C. HOSPITAL INFORMATION SYSTEMS: AN AUTOMATED TUMOR REGISTRY

At the Massachusetts Memorial Hospitals of the Boston University Medical Center we have undertaken the design and implementation of an automated Tumor Registry system. It is planned that this system will be readily accessible for administrative, medical, and research use by hospital personnel. The present Tumor Registry is contained in folders and file cabinets and has proved inadequate for the demands of the hospital community. The new system (Fig. XX-13) will be organized around an IBM 1620 digital computer and will use conventional hospital records and the Termatrex Information System. This report describes the organization and programming of an initial pilot system for the Tumor Registry.

The basic components consist of an IBM Model II 1620 computer with 60,000 memory cores, punched card and typewriter input/output, and a 1311 disk storage drive. The computer is equipped with the Monitor I executive routine. The Termatrex System

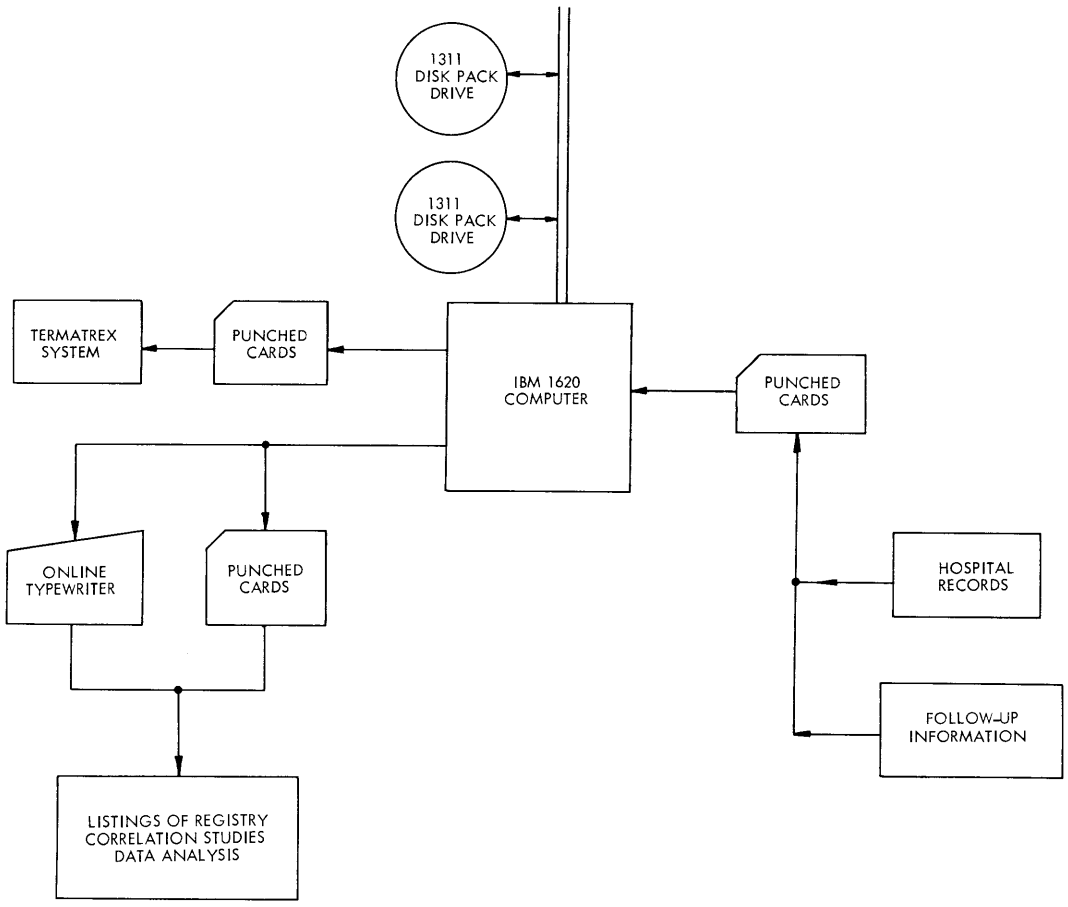

Fig. XX-13. Automated tumor registry system.

is a hand-operated, cross-referenced filing system; by assigning predetermined codes to the various characteristics of a case history, it can accommodate several hundred characteristics of as many as 10,000 patients.

The computer serves as a clearing house and storage area for the Tumor Registry. All information entering the Registry initially passes through the computer, where three types of processing occur. First, the Model 1620 checks the data for errors; for example, a birth date of June, 1967 is an obvious mistake; less obvious errors might be the incorrect spelling of a diagnosis or a nonexistent type of medication. When the data have passed the error-check routine the computer matches each item of the patient's record with the appropriate Termatrex code. The code is then output immediately on punched cards or directly on the 1620's on-line typewriter. The third processing function is storage of the information on the disk pack. This constitutes the actual entry of information into the Registry. Before storage, the data are broken down into two major categories, initial data and subsequent or follow-up data. These categories conform to the pattern of the conventional hospital record and provide a convenient way of organizing the Registry on the disk.

For the pilot system there are approximately 20 terms describing the initial condition of a tumor, and 8 terms for each follow-up report. The initial data are stored at the front of the disk pack and arranged in sequential tables with one table for each term. Follow-up data for each tumor are stored as a pointer list, starting directly after the last entry of the initial data tables. Theoretically, there is no upper limit to the number of tumor cases that can be stored in the completed Registry, as more disk packs can be added to increase its capacity. The pilot system's size, however, is now limited to 1008 cases, as this number can be easily handled on one disk pack, and, at the same time, is large enough to permit a thorough debugging of the system.

The system is augmented by several main programs, corresponding to the major functions of the system, such as data storage, updating, and information retrieval. Figure XX-14 shows the organization of the data-storage program. The main program is a control program; it keeps track of which data has been processed and which subprogram is next to be executed. Each subprogram processes one item of the input record. During execution, control passes from the main program to a subprogram, back to the main program, and then on to another subprogram. The subprograms are completely independent of each other and can be executed in any order and any number of times for each case input. Part of the data of each input record is a code telling the main program the order in which the subprograms are to be executed to process that input record.

This structure permits great flexibility in deciding which characteristics should be recorded in the system. If a new term must be added to each patient's record, a new subprogram is written and added to the rest. Space on the disk pack for storing the new

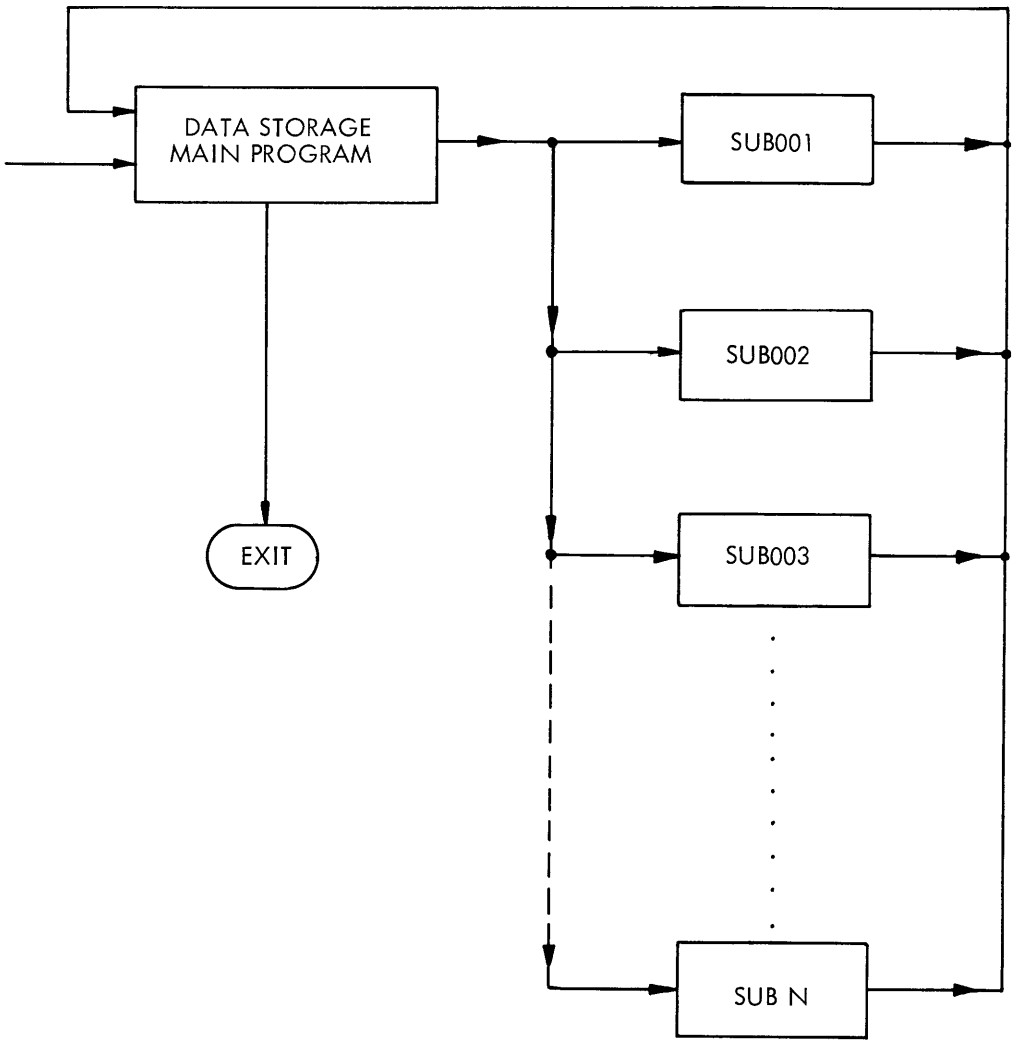

Fig. XX-14. Data-storage programs.

term can be procured either by copying the entire disk onto another disk and leaving an appropriate amount of blank space between the previous last initial data table and the first follow-up data, or by isolating a block of space in the follow-up data area.

The actual method of entering data into the Tumor Registry is still rather primitive. The pertinent data are abstracted from the patient's record, keypunched in a standard abbreviated form, and then introduced into the Model 1620. When the total system is operational, it should be possible to set up a direct communication link from data-collection points to the computer through a time-sharing system teletype; this would permit either an abstracter or a physician to enter the data directly into the Registry. Use of such a system for entering the data would greatly facilitate updating of the Registry.

Information retrieval is, of course, the major goal of a computerized Tumor Registry. For example, the computer can produce, in a very short time, a listing of the entire Registry of the patients who are due for follow-up visits in a given month, or of patients with more than one primary tumor. It readily allows comparisons to be made of the results of a similar treatment of different tumors, of survival times of patients with tumors in various stages of growth or of the frequency with which a clinical diagnosis is confirmed by histological evidence. Because the information is stored essentially by characteristic and not by patient, the search time for a given set of characteristics is minimal.

The work, thus far, has been concerned with laying out the format of the disk pack, comparing various methods of data storage, and coding initial data-storage programs. The disk pack format is being designed for the entire group of initial and follow-up terms, and data-storage subprograms are being coded for all of these terms.

T. Ostrand, J. F. Dickson

D. INTERPRETIVE AND DIAGNOSTIC MATRICES FOR COMPUTER DIAGNOSIS OF ELECTROCARDIOGRAMS

1. Introduction

Figure XX-15 is a block diagram of the operational sequence in a computer system designed for remote on-line, real-time diagnosis of clinical electrocardiograms (EKG). In operation, an executive monitor which is used by a hospital technician for remote control of the sequence of operations, is placed in the G. E. 225 computer in the laboratory of the Neurology Group at the Massachusetts Institute of Technology. The diagnostic process is then begun by the hospital technician with the telephone line transmission of a patient's identifying data and EKG signals to the computer.

The EKG signals originating in the hospital are often obscured by noise, and preprocessing is necessary to facilitate rhythm interpretation, pattern recognition, and parameter extraction. The rhythm section, analyzing the atrial and ventricular rates and prematurities, yields approximately 20 mutually exclusive, tentative, rhythm interpretations. In the morphological identification section of the program, the current filters analyze the X-lead of Frank's orthogonal lead system. The P, QRS, and ST-T segments of the EKG signal are introduced to adaptive matched-filter pattern-recognition programs that provide tentative pattern-recognition interpretations. Following point recognition, the parameter-extracting portion of the program makes pertinent determinations that relate to amplitude (as amplitude of the QRS complex) and interval (as the Q-T interval).

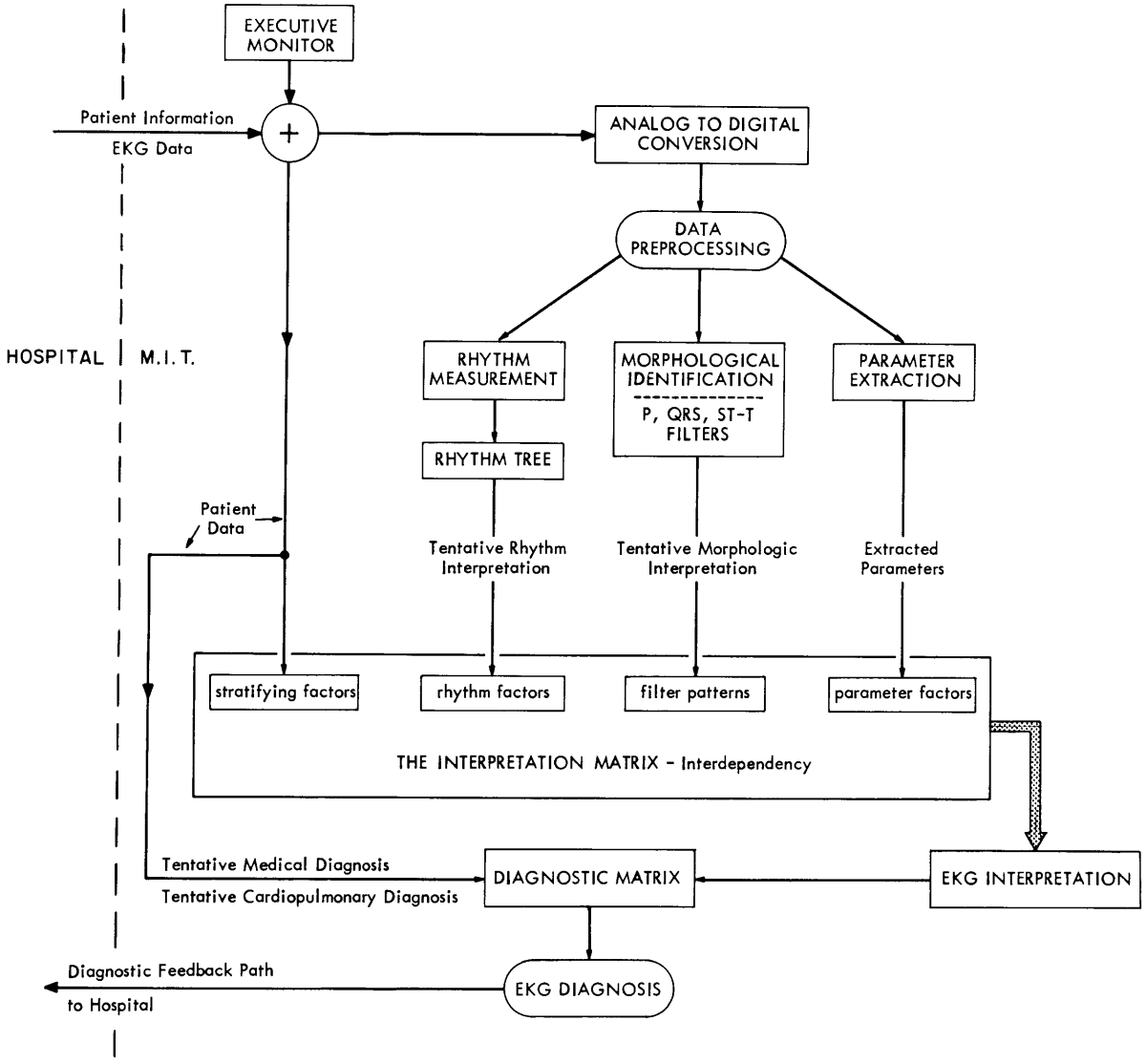

Fig. XX-15. Sequence of the diagnostic system.

2. Interpretive and Diagnostic Matrices

In this part of the diagnostic sequence the independently determined rhythm, pattern recognition, amplitude, and duration parameters are allowed to interrelate for the first time in an additive pattern-recognition matrix. Stratifying factors, such as age, sex, ponderal index, drugs, etc. are also admitted to the diagnostic sequence at this point in the program. Fixed weightings are assigned for the various diagnostic criteria either arbitrarily or adaptively by a learning matrix technique. This matrix yields 25 EKG interpretations (Fig. XX-16), in addition to the rhythm interpretations mentioned above.

1. Within normal limits
2. Left ventricular hypertrophy
3. Right ventricular hypertrophy
4. Complete left bundle branch block
5. Incomplete left bundle branch block
6. Complete right bundle branch block
7. Incomplete right bundle branch block
8. Intraventricular block
9. Acute myocardial infarction
10. Anteroseptal myocardial infarction
11. Inferior myocardial infarction
12. Lateral myocardial infarction
13. Digitalis effect
14. Digitalis intoxication
15. Hyperkalemia
16. Hypokalemia
17. Hypocalcemia
18. Nonspecific ST-T abnormalities
19. Marked ST depression
20. Pericarditis
21. Left atrial hypertrophy
22. Right atrial hypertrophy
23. Acute cor pulmonale
24. Chronic cor pulmonale
25. Wolff-Parkinson-White syndrome

Fig. XX-16. Twenty-five EKG interpretations contained in the interpretation matrix.

These findings are returned by telephone line for display by teletype at the hospital laboratory.

In the course of reading electrocardiograms one essentially looks for or encounters many information points and then sums their contribution over a decision area for a final diagnosis. We have developed this weighted additive matrix to operate somewhat similarly. It is an adaptive, linear model that accepts nonbinary, probabilistic inputs, does not require that its outputs (diagnoses) be independent, and can display straightforward numerical reasons for its decisions. This matrix now has 174 rows and 25 columns. The rows are divided into 43 categories relating to four types of data: (i) stratified clinical information, such as age, height, weight, sex, and electrocardiographically important drugs being taken, (ii) tentative rhythm analyses, (iii) tentative adaptive matched-filter interpretations, and (iv) the resultant findings of the parameter extraction program. The columns represent the 25 commonly encountered EKG interpretations that have been selected from a frequency table of diagnoses made in the EKG laboratory of the Massachusetts Memorial Hospitals in the years 1961-1962.

The values used to fill the matrix may range from -500 to +500, a negative value indicating that a particular entry in the matrix weights negatively in the determination of a particular interpretation, as with a short QRS duration for bundle branch block. Zero entries indicate that the information does not contribute to a decision. For the filters the assigned weighted number for pattern recognition is multiplied by the determined correlation coefficient, though it is not clear at this time that the correlation coefficient should necessarily modify the weighted number linearly. Originally, the matrix values were assigned arbitrarily on the basis of clinical experience; however, a self-learning program for the matrix now makes use of our EKG library to refine these values. In the calculation process a patient vector is created, each element of which corresponds to a specific row of the matrix. In each case, except for the filters,

a coefficient of 0 or 1 is assigned as is appropriate. For the filters the correlation coefficient is used. The patient vector is multiplied by the matrix, after which each column is summed to yield 25 additive interpretation totals. Since even the largest sum may represent an unlikely interpretation, the final step is to establish a "certainty" normalization for these interpretation totals. This is done as follows. A maximum possible value for each category is +500. An interpretation of maximum certainty would give a column total equal to the sum of the exhibited patient vector coefficients multiplied by 500 for an ideal sum. Accordingly, the sum of each column is divided by the ideal sum, and yields a certainty factor between minus one and plus one for each interpretation. The interpretation and diagnostic matrices are similarly constructed, so that the final output of the system is an EKG diagnosis with a certainty factor. A means for the automatic adjustment of weightings by a "self-learning" routine is available.

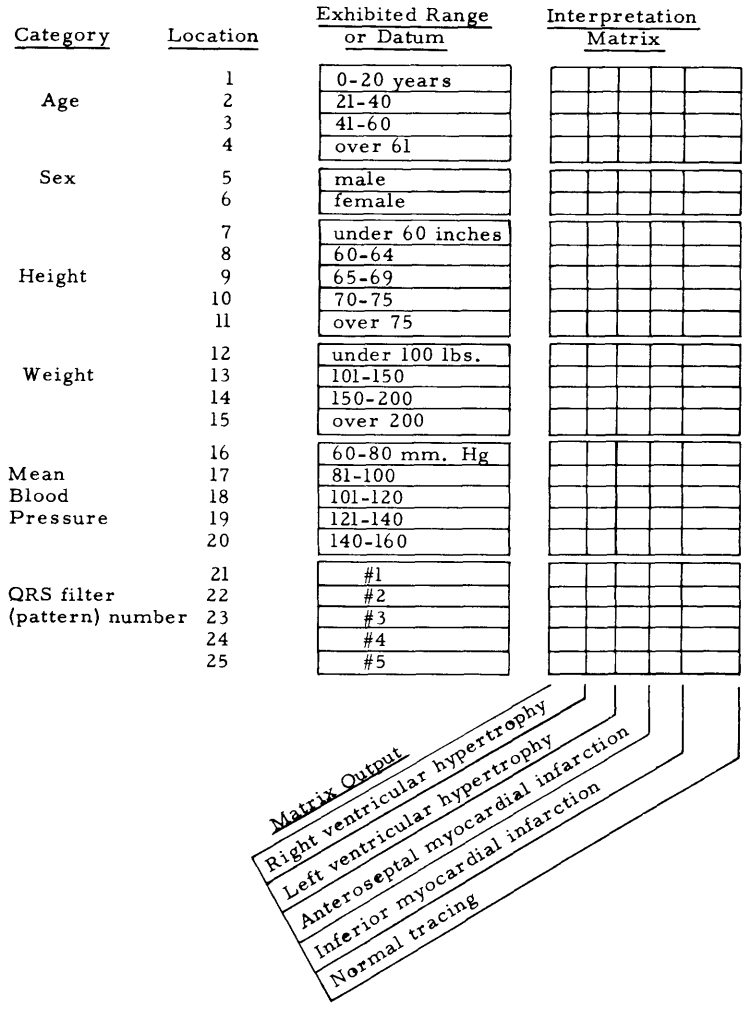

Fig. XX-17. Abbreviated interpretation matrix.

It reinforces or negatively reinforces appropriate matrix elements, since data from a patient with a known EKG interpretation are passed through, the outcome depending on whether the matrix arrives at a correct or an incorrect interpretation.

The approach just outlined is demonstrated by the following example (Fig. XX-17). The input data for a given patient are entered in the appropriate locations (rows) of a column vector whose potential entries correspond exactly to the named entries (rows) of the interpretation matrix. Most of this information is in the form of graded categories. The rows are labeled with respect to the patient's age, height, mean blood pressure, weight, sex, and type of electrocardiographic pattern.

The matrix on the right side of the figure can yield only five interpretations in this instance (the result has been abbreviated here for pedagogical purposes). When the data on a given patient are entered in the column vector on the left, the corresponding rows of the matrix become operational; that is, the weighting coefficients in the rows to which the patient has contributed data are selected for the diagnostic summing process. For a male patient, 25 years old, whose height is 68 inches, weight 162 lbs, mean blood pressure 98 mm mercury, and whose electrocardiographic QRS complex most closely resembles the pattern of filter No. 2, the rows 2, 5, 9, 14, 17, and 22 of the matrix would become operational. The weighting coefficients located in each cell of these rows would then be summed for each of the 5 diagnostic columns of the matrix. The interpretation assigned to the column with the largest sum would then be output as the most likely interpretation, together with a "certainty coefficient" that would indicate the likelihood of its correctness (in this case the sum of the observed coefficients divided by 12,500).

In the case of the "learning matrix," each cell in every row and column of the matrix would initially be zero. Consequently, when the very first patient was put through, the sum in each column would be zero and all five diagnoses would be equally possible. For this case, an arbitrary tie-breaking decision has been assigned: the machine is instructed to take the leftmost diagnostic column in case of ties and consider that to be the diagnosis. Our hypothetical first patient would thus be given the diagnosis of "right ventricular hypertrophy" (column 1).

Suppose, however, that his correct diagnosis as established clinically was "normal tracing" (column 5). During the matrix learning process, this correct answer would also have been entered in thecomputer. A comparison between the correct answer and the answer given by the matrix would be made. In case of a discrepancy, such as that just outlined, all of the operational entries in the right ventricular hypertrophy column would be negatively reinforced by subtracting an arbitrary amount from those weighting coefficients. Similarly, all operational entries in the 5th column would be reinforced by addition of the same amount as was previously subtracted in the "punishing" routine. The "punishment" and "reward" would be equalized in this way, to prevent the numerical value of the matrix as a whole from drifting off-scale. The average value of the

matrix at all times would thus be equal to zero. If this sequence were frequently repeated by processing many patients with known diagnoses, the matrix of weighting coefficients would ideally converge toward the situation wherein the individual entries would have a meaning analogous to conventional statistical discriminant function coefficients.

The advantages of the present "adaptive" scheme are its greater convenience (automaticness) and its open-ended quality. By the last we mean that the stored matrix can be improved at any time without having to destroy the current matrix and start afresh each time a new group of patients with known diagnoses is to be processed. On the other hand, with the learning matrix scheme outlined above, the matrix in its current state can be used to interpret unknown tracings at any time by operating in a fixed, nonlearning form.

For research purposes, the interpretation matrix must contain various indexing and bookkeeping rows and columns that keep track of the types of previously diagnosed electrocardiograms entering into the adaptive matrix, the number of the various clinical input and filter parameters actually utilized, and a tally with respect to the number of correct matrix interpretations and normalizing factors giving estimates of the validity of the weighting coefficients in the matrix at any given time. It will thus be possible to assess quantitatively, perhaps for the first time in extenso, the importance of various clinical and morphologic characteristics for a given interpretation.

J. F. Dickson, D. Martin, G. H. Whipple